

# Analytical sensitivity and efficiency comparisons of SARS-CoV-2 qRT-PCR assays

Chantal B.F. Vogels<sup>1\*</sup>, Anderson F. Brito<sup>1</sup>, Anne L. Wyllie<sup>1</sup>, Joseph R. Fauver<sup>1</sup>, Isabel M. Ott<sup>2</sup>, Chaney C. Kalinich<sup>1</sup>, Mary E. Petrone<sup>1</sup>, Arnau Casanovas-Massana<sup>1</sup>, M. Catherine Muenker<sup>1</sup>, Adam J. Moore<sup>1</sup>, Jonathan Klein<sup>3</sup>, Peiwen Lu<sup>3</sup>, Alice Lu-Culligan<sup>3</sup>, Xiaodong Jiang<sup>3</sup>, Daniel J. Kim<sup>3</sup>, Eriko Kudo<sup>3</sup>, Tianyang Mao<sup>3</sup>, Miyu Moriyama<sup>3</sup>, Ji Eun Oh<sup>3</sup>, Annsea Park<sup>3</sup>, Julio Silva<sup>3</sup>, Eric Song<sup>3</sup>, Takehiro Takahashi<sup>3</sup>, Manabu Taura<sup>3</sup>, Maria Tokuyama<sup>3</sup>, Arvind Venkataraman<sup>3</sup>, Orr-El Weizman<sup>3</sup>, Patrick Wong<sup>3</sup>, Yexin Yang<sup>3</sup>, Nagarjuna R. Cheemarla<sup>4</sup>, Elizabeth B. White<sup>1</sup>, Sarah Lapidus<sup>1</sup>, Rebecca Earnest<sup>1</sup>, Bertie Geng<sup>5</sup>, Pavithra Vijayakumar<sup>5</sup>, Camila Odio<sup>6</sup>, John Fournier<sup>7</sup>, Santos Bermejo<sup>8</sup>, Shelli Farhadian<sup>7</sup>, Charles S. Dela Cruz<sup>8</sup>, Akiko Iwasaki<sup>3,9</sup>, Albert I. Ko<sup>1</sup>, Marie L. Landry<sup>4,7,10</sup>, Ellen F. Foxman<sup>3,4</sup>, Nathan D. Grubaugh<sup>1\*</sup>

<sup>1</sup> Department of Epidemiology of Microbial Diseases, Yale School of Public Health, New Haven, CT 06510, USA

<sup>2</sup> Department of Ecology and Evolutionary Biology, Yale University, New Haven, CT 06520, USA

<sup>3</sup> Department of Immunobiology, Yale University School of Medicine, New Haven, CT, 06510, USA

<sup>4</sup> Department of Laboratory Medicine, Yale University School of Medicine, New Haven, CT, 06510, USA

<sup>5</sup> Department of Obstetrics, Gynecology, and Reproductive Sciences, Yale University School of Medicine, New Haven, CT, 06510, USA

<sup>6</sup> Department of Medicine, Northeast Medical Group, Yale-New Haven Health, New Haven, CT 06510, USA

<sup>7</sup> Department of Medicine, Section of Infectious Diseases, Yale University School of Medicine, New Haven, CT, 06510, USA

<sup>8</sup> Department of Internal Medicine, Section of Pulmonary, Critical Care, and Sleep Medicine, Yale School of Medicine, New Haven, CT, 06510, USA

<sup>9</sup> Howard Hughes Medical Institute, Chevy Chase, Maryland 20815, USA

<sup>10</sup> Clinical Virology Laboratory, Yale-New Haven Hospital, New Haven, CT, 06510, USA

\* Correspondence: [chantal.vogels@yale.edu](mailto:chantal.vogels@yale.edu) (CBFV); [nathan.grubaugh@yale.edu](mailto:nathan.grubaugh@yale.edu) (NDG)

## Abstract

The recent spread of severe acute respiratory syndrome coronavirus 2 (SARS-CoV-2) exemplifies the critical need for accurate and rapid diagnostic assays to prompt clinical and public health interventions. Currently, several quantitative reverse-transcription polymerase chain reaction (qRT-PCR) assays are being used by clinical, research, and public health laboratories. However, it is currently unclear if results from different tests are comparable. Our goal was to evaluate the primer-probe sets used in four common diagnostic assays available on the World Health Organization (WHO) website. To facilitate this effort, we generated RNA transcripts to be used as assay standards and distributed them to other laboratories for internal validation. We then used these (1) RNA transcript standards, (2) full-length SARS-CoV-2 RNA, and (3) pre-COVID-19 nasopharyngeal swabs, and (4) clinical samples from COVID-19 patients to determine analytical efficiency and sensitivity of the qRT-PCR primer-probe sets. We show that all primer-probe sets can be used to detect SARS-CoV-2, but there are clear differences in the ability to differentiate between true negatives and positives with low amounts of virus. We found that several primer-probe sets cross-react with SARS-CoV-2-negative nasopharyngeal swabs. However, background cross-reactivity by the 2019-nCoV\_N2 set issued by the US Centers for Disease Control and Prevention did not interfere with outcomes of the combined “N1” and “N2” assay when testing COVID-19 clinical samples. Our findings characterize the limitations of currently used

primer-probe sets and can assist other laboratories in selecting appropriate assays for the detection of SARS-CoV-2.

## Introduction

Accurate diagnostic assays and large-scale testing are critical for mitigating outbreaks of infectious diseases. Early detection prompts public health actions to prevent and control the spread of pathogens. This has been exemplified by the novel coronavirus, known as SARS-CoV-2, which was first identified as the cause of an outbreak of pneumonia in Wuhan, China, in December 2019, and rapidly spread around the world<sup>1-3</sup>. The first SARS-CoV-2 genome sequence was critical for the development of diagnostics<sup>2</sup>, which led to several molecular assays being developed to detect COVID-19 cases<sup>4-7</sup>. The World Health Organization (WHO) currently lists seven molecular assays (i.e. qRT-PCR) to diagnose COVID-19<sup>8</sup>; however, it is not clear to many laboratories or public health agencies which assay they should adopt.

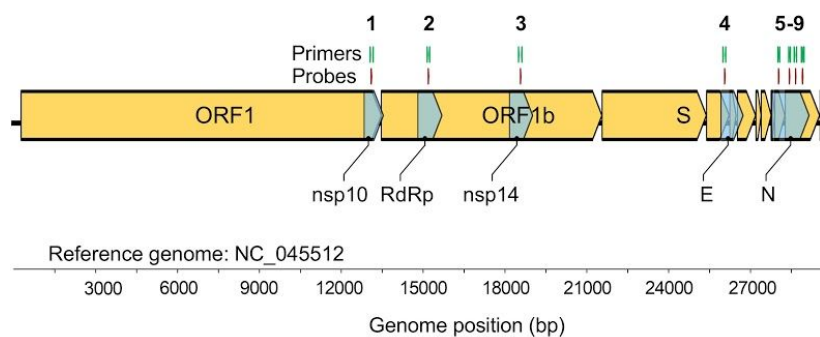
Our goal was to compare the analytical efficiencies and sensitivities of the four most common SARS-CoV-2 qRT-PCR assays developed by the China Center for Disease Control (China CDC)<sup>7</sup>, United States CDC (US CDC)<sup>6</sup>, Charité Institute of Virology, Universitätsmedizin Berlin (Charité)<sup>5</sup>, and Hong Kong University (HKU)<sup>4</sup>. To this end, we first generated RNA transcripts from a SARS-CoV-2 isolate from an early COVID-19 case from the state of Washington (United States)<sup>9</sup>. Using RNA transcripts, isolated SARS-CoV-2 RNA, pre-COVID-19 nasopharyngeal swabs, and clinical samples from COVID-19 patients, we find differences between the analytical sensitivities to detect low amounts of SARS-CoV-2 and the detection of false positives. Thus, we provide limitations for many of the qRT-PCR primer-probe sets that should be considered when using these assays.

## Results

### Generation of RNA transcript standards for qRT-PCR validation

A barrier to implementing and validating qRT-PCR molecular assays for SARS-CoV-2 detection was the availability of virus RNA standards. As the full length SARS-CoV-2 RNA is considered as a biological safety level 2 hazard in the US, we generated small RNA transcripts (704-1363 nt) from the non-structural protein 10 (nsp10), RNA-dependent RNA polymerase (RdRp), non-structural protein 14 (nsp14), envelope (E), and nucleocapsid (N) genes spanning each of the primer and probe sets in the China CDC<sup>7</sup>, US CDC<sup>6</sup>, Charité<sup>5</sup>, and HKU<sup>4</sup> assays (**Fig. 1A**; **Table 1**; **Supplemental Tables 1-2**)<sup>10</sup>. By measuring PCR amplification using 10-fold serial dilutions of our RNA transcript standards, we found the efficiencies of each of the nine primer-probe sets to be above 90% (**Fig. 1B**), which match the criteria for an efficient qRT-PCR assay<sup>11</sup>. Our RNA transcripts can thus be used for assay validation, positive controls, and standards to quantify viral loads: critical steps for a diagnostic assay. Our protocol to generate the RNA transcripts is openly available<sup>10</sup>, and any clinical or research diagnostic lab can directly request them for free through our lab website ([www.grubaughlab.com](http://www.grubaughlab.com)).

**A**



**B**

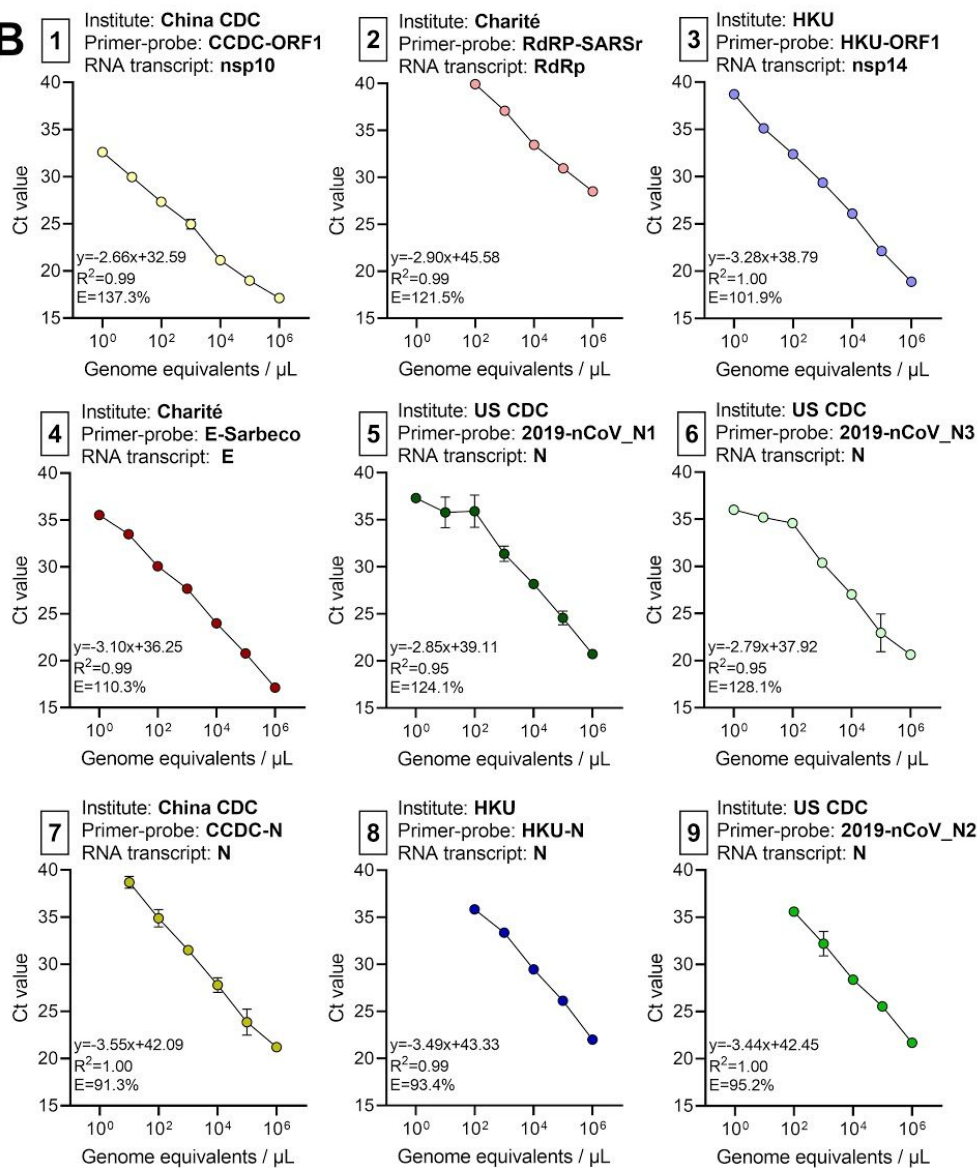


**Fig. 1: Generation of RNA transcript standards for validation of SARS-CoV-2 qRT-PCR assays.**

(A) We reverse-transcribed RNA transcript standards for the non-structural protein 10 (nsp10), RNA-dependent RNA polymerase (RdRp), non-structural protein 14 (nsp14), envelope (E), and nucleocapsid (N) genes to be used for validation of nine primer-probe sets used in SARS-CoV-2 qRT-PCR assays. (B) We generated standard curves for nine primer-probe sets with 10-fold dilutions

( $10^0$ - $10^6$  genome equivalents/ $\mu$ L) of the corresponding RNA transcript standards. For each combination of primer-probe set and RNA transcript standard, we provide the slope, intercept,  $R^2$ , and efficiency. The primer-probe sets are numbered as shown in panel A.

**Table 1: Primers and probes for common SARS-CoV-2 qRT-PCR diagnostic assays.**

Institute	Target	Primer/Probe	Sequence	Ref
Charité	E	E_Sarbeco_F	ACAGGTACGTTAATAGTTAATAGCGT	5
		E_Sarbeco_R	ATATTGCAGCAGTACGCACACA	
		E_Sarbeco_P1	FAM-ACACTAGCCATCCTTACTGCGCTTCG-BHQ1	
	RdRp	RdRp_SARSr-F	GTGAR <b>AT</b> GGTCATGTGTGGCGG	
		RdRp_SARSr-R	CARATGTTAA <b>S</b> ACTATTAGCATA	
		RdRp_SARSr-P1	FAM-CCAGGTGG <b>W</b> AC <b>R</b> TCATC <b>M</b> GGTGATGC-BHQ1	
RdRp_SARSr-P2	FAM-CAGGTGGAACCTCATCAGGAGATGC-BHQ1			
HKU	N	HKU-N-F	TAATCAGACAAGGA <b>A</b> CTGATTA	4
		HKU-N-R	CGAAGGTGTGACTTCCATG	
		HKU-N-P	FAM-GCAAATTGTGCAATTTGCGG-BHQ1	
	nsp14	HKU-ORF1-F	TGGGGYTTTACRGGTAACCT	
		HKU-ORF1-R	AAC <b>R</b> CGCTTAACAAAGCACTC	
		HKU-ORF1-P	FAM-TAGTTGTGATGC <b>W</b> ATCATGACTAG-BHQ1	
China CDC	N	CCDC-N-F	GGGGA <b>A</b> CTTCTCCTGCTAGAAT	7
		CCDC-N-R	CAGACATTTTGTCTCAAGCTG	
		CCDC-N-P	FAM-TTGCTGCTGCTTGACAGATT-BHQ1	
	nsp10	CCDC-ORF1-F	CCCTGTGGGTTTTACTTAA	
		CCDC-ORF1-R	ACGATTGTGCATCAGCTGA	
		CCDC-ORF1-P	FAM-CCGTCTGCGGTATGTGGAAAGTTATGG-BHQ1	
US CDC	N	2019-nCoV_N1-F	GACCCCAA <b>A</b> ATCAGCGAAAT	6
		2019-nCoV_N1-R	TCTGGTACTGCCAGTTGAATCTG	
		2019-nCoV_N1-P	FAM-ACCCCGCATTACGTTTGGTGGACC-BHQ1	
	N	2019-nCoV_N2-F	TTACAAACATTGGCCGCAA	
		2019-nCoV_N2-R	GCGCGACATTCCGAAGAA	
		2019-nCoV_N2-P	FAM-ACAATTTGCCCCAGCGCTTCAG-BHQ1	
	N	2019-nCoV_N3-F	GGGAGCCTTGAATACACCAAAA	
		2019-nCoV_N3-R	TGTAGCACGATTGCAGCATTG	
		2019-nCoV_N3-P	FAM-AYCACATTGGCACCCGCAATCCTG-BHQ1	
	Human RNase P	RP-F	AGATTTGGACCTGCGAGCG	
		RP-R	GAGCGGCTGTCTCCACAAGT	
		RP-P	FAM-TTCTGACCTGAAGGCTCTGCGCG-BHQ1	

Degenerate nucleotides are shown in bold.

### Analytical comparisons of qRT-PCR primer-probe sets

Critical evaluations of the designed primer-probe sets used in the primary SARS-CoV-2 qRT-PCR detection assays are necessary to compare findings across studies, and select

appropriate assays for in-house testing. The goal of our study was to compare the designed primer-probe sets, not the assays *per se*, as that would involve many different variables. To do so we used the same (1) primer-probe concentrations (500 nM of forward and reverse primer, and 250 nM of probe); (2) PCR reagents (New England Biolabs Luna Universal One-step RT-qPCR kit); and (3) thermocycler conditions (40 cycles of 10 seconds at 95°C and 20 seconds at 55°C) in all reactions. From our measured PCR amplification efficiencies and analytical sensitivities of detection, most primer-probe sets were comparable, except for the RdRp-SARSr (Charité) set, which had low sensitivity (Fig. 2).

By testing each of the nine primer-probe sets using 10-fold dilutions of SARS-CoV-2 RNA derived from cell culture (Fig. 2A) or 10-fold dilutions of SARS-CoV-2 RNA spiked into RNA extracted from pooled nasopharyngeal swabs taken from patients in 2017 (SARS-CoV-2 RNA-spiked mocks; Fig. 2B), we again found that the PCR amplification efficiencies were near or above 90% (Fig. 2C). To measure the analytical sensitivity of virus detection, we used the cycle threshold (Ct) value in which the expected linear dilution series would cross the y-intercept when tested with 1 genome equivalent per  $\mu\text{L}$  of RNA. Our measured sensitivities (y-intercept Ct values) were similar among most of the primer-probe sets, except for the RdRp-SARSr (Charité) set (Fig. 2D). We found that the Ct values from the RdRp-SARSr set were usually 6-10 Cts higher (lower virus detection) than the other primer-probe sets.

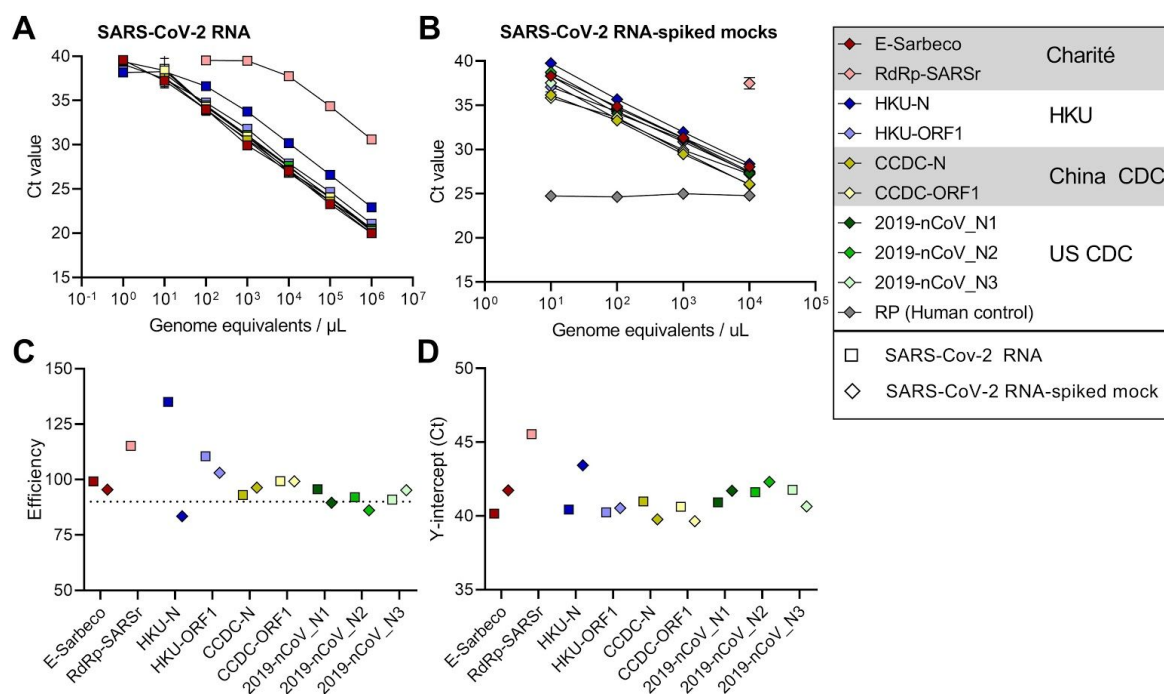


**Fig. 2: Analytical efficiency and sensitivity of the nine primer-probe sets used in SARS-CoV-2 qRT-PCR assays.** We compared nine primer-probe sets and a human control primer-probe set targeting the human RNase P gene with 10-fold dilutions of (A) full-length SARS-CoV-2 RNA and (B) pre-COVID-19 mock samples spiked with known concentrations of SARS-CoV-2 RNA. We determined (C) efficiency and (D) y-intercept Ct values (measured analytical sensitivity) of the nine primer-probe sets. We extracted nucleic acid from SARS-CoV-2-negative nasopharyngeal swabs (collected from respiratory disease patients in 2017) and spiked these with known concentrations of

SARS-CoV-2 RNA. Symbols depict sample types: squares represent tests with SARS-CoV-2 RNA and diamonds represent SARS-CoV-2 RNA-spiked mock samples. Colors depict the nine tested primer-probe sets. The CDC human RNase P (RP) assay was included as an extraction control.

### Detection of virus at low concentrations and false positives

To determine the lower limit of detection and the occurrence of false positive or inconclusive detections, we tested the primer-probe sets using SARS-CoV-2 RNA spiked into RNA extracted from pooled nasopharyngeal swabs from respiratory disease patients during 2017 (pre-COVID-19). Our mock clinical samples demonstrated that many of the primer-probe sets cross-reacted with non-SARS-CoV-2 nucleic acid, which may lead to inconclusive or false positive results (**Fig. 3**).

When testing nasopharyngeal swabs collected prior to the COVID-19 pandemic, we found that qRT-PCR with five primer-probe sets did not result in background amplification (E-Sarbeco, RdRp-SARsR, HKU-N, HKU-ORF1, and 2019-nCoV\_N1; **Fig. 3**). When using SARS-CoV-2 RNA spiked into RNA from these nasopharyngeal swabs, our results show that none of these five primer-probe sets were able to detect (Ct values <40) SARS-CoV-2 RNA at 1 ( $10^0$ ) virus genome equivalents/ $\mu$ L and all could partially detect 10 ( $10^1$ ) virus genome equivalents/ $\mu$ L (**Fig. 3**). Our results suggest that the two most sensitive primer-probe sets are E-Sarbeco (Charité) and HKU-ORF1 (HKU), which each detected 6/8 (75%) of the nasopharyngeal swabs spiked with 10 virus genome equivalents/ $\mu$ L (**Fig. 3**). At 100 ( $10^2$ ) virus genome equivalents/ $\mu$ L, we could detect virus and differentiate between the negative samples for all replicates and primers sets, except for the RdRp-SARsR (Charité) set, which was negative (Ct values >40) for all  $10^0$ - $10^2$  genome equivalents/ $\mu$ L concentrations.

We detected amplification of nonspecific products (Ct values <40) from nasopharyngeal swabs collected prior to the COVID-19 pandemic for the CCDC-N (5/8, 62.5%), CCDC-ORF1 (2/8, 25%), 2019-nCoV\_N2 (2/8, 25%), and 2019-nCoV\_N3 (6/8, 75%; **Fig. 3**). Moreover, the Ct value ranges for SARS-CoV-2-negative samples overlapped with the Ct value ranges (~36-40) for the swabs spiked with  $10^0$  and  $10^1$  SARS-CoV-2 genome equivalents/ $\mu$ L (**Fig. 3**). Our data indicates that the background cross-reactivity that we observed may limit the ability to differentiate between true positives and negatives at SARS-CoV-2 concentrations at or below 10 virus genome equivalents/ $\mu$ L when using the CCDC-N, CCDC-ORF1, 2019-nCoV\_N2, and 2019-nCoV\_N3. In fact, the 2019-nCoV\_N3 primer-probe set has been excluded from the US CDC assay due to these issues<sup>12</sup>. However, Casto *et al.* also compared several SARS-CoV-2 primer-probe sets by testing dilutions of clinical samples and they did not detect any cross-reactivity for the 2019-nCoV\_N2 set<sup>13</sup>. The source of the background cross-reactivity is unclear at present, but it may be attributable to non-specific detection of other seasonal coronaviruses that were circulating in 2017.

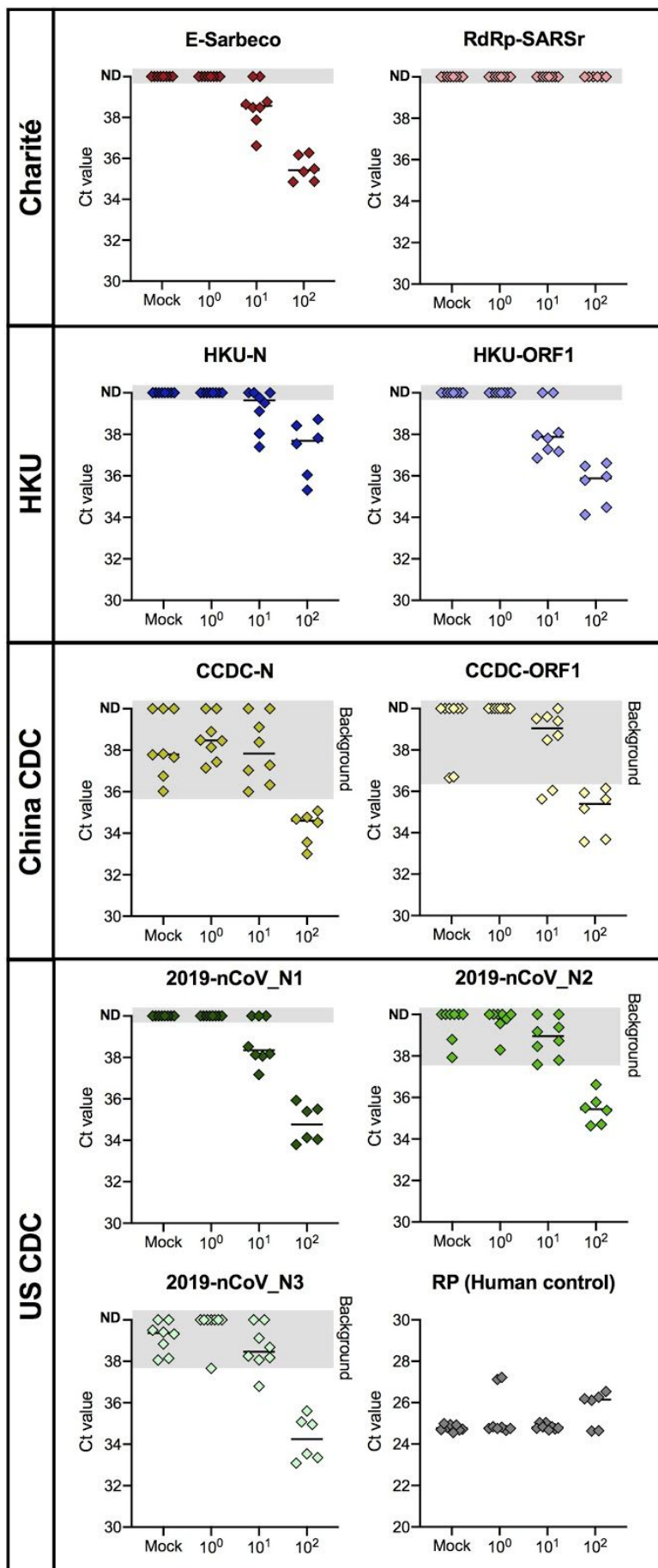


**Fig. 3: All nine primer-probe sets have a similar lower detection limit of  $10^2$  SARS-CoV-2 genome equivalents/ $\mu$ L.** We determined the lower detection limit of nine primer-probe sets as well as the human RNase P control for mock samples (RNA extracted from nasopharyngeal swabs collected in 2017) spiked with known concentrations of SARS-CoV-2 RNA. We performed 6-8 technical replicates with mock samples without spiking RNA and mock samples spiked with  $10^0$ - $10^2$  genome equivalent/ $\mu$ L of SARS-CoV-2 RNA. For each primer-probe set, we show the range of cycle threshold values obtained with mock samples extracted from SARS-CoV-2-negative nasopharyngeal swabs, which indicates variation in the lower detection limit of each primer-probe set. ND = not detected. Gray-shaded areas = non-specific amplification.

### **Non-specific amplification does not affect outcome of US CDC assay**

To investigate if the background cross-reactivity with pre-COVID-19 nasopharyngeal swabs that we observed for the US CDC 2019-nCoV\_N2 primer-probe set (**Fig. 3**) would impact the testing outcomes of the US CDC assay, we compared 2019-nCoV\_N1 and N2 results from 172 clinical samples taken during the COVID-19 pandemic (**Fig. 4**). We found that N1 was typically more sensitive, yielding lower Ct values from positive samples, and that background cross-reactivity with N2 did not yield an abundance of inconclusive test results.

Using nasopharyngeal swabs, saliva, urine, and rectal swabs from patients enrolled in our COVID-19 research protocol at the Yale-New Haven Hospital, we found that more samples had lower Ct values (more efficient virus detection) using the 2019-nCoV\_N1 primer-probe set as compared to 2019-nCoV\_N2 (**Fig. 4A**). Interestingly, with the N1 set, samples with a Ct value of approximately 40 and samples that were not detected (ND) were clearly discrete groups, whereas several samples that were not detected by the N1 set were in the 41-43 Ct range for the N2 set (**Fig. 5B**). This further supports our observation that the US CDC 2019-nCoV\_N2 primer-probe set produces some non-specific amplification. However, when we look at the US CDC assay outcomes, which take into account both the N1 and N2 results, only 1 out of 172 tests was deemed inconclusive due to N1 being negative ( $>40$  Ct) and N2 being positive ( $<40$  Ct) due to non-specific amplification (**Fig. 5C**). When a more stringent Ct value cut-off of 38 was implemented, we did not detect any inconclusive results where N2 was the only positive set. In fact, we found more inconclusive results where N1 was the only positive set at both 40 Ct (3/172) and 38 Ct (5/172) cut-offs (**Fig. 5C**), likely because the 2019-nCoV\_N1 primer-probe set is more sensitive (**Figs. 4, 5A, 5B**). Overall, we generated inconclusive results from less than 3% of the tested clinical samples using the US CDC primer-probe sets, indicating that background cross-reactivity does not have a large impact on the testing outcomes.



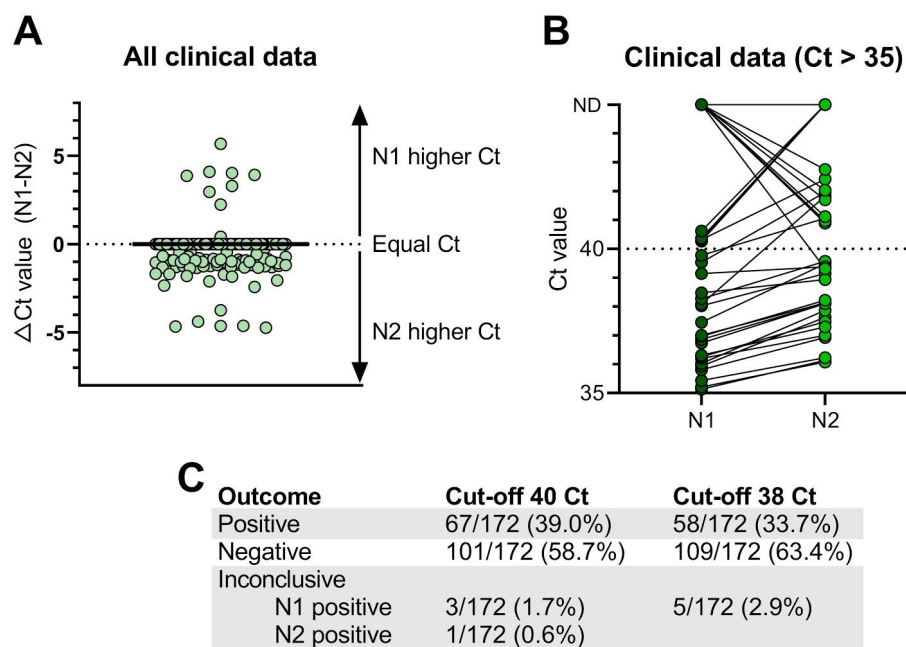


**Fig. 4: Background cross-reactivity does not affect the testing outcomes when using the US CDC N1 and N2 primer-probe sets.** We compared Ct values for clinical samples obtained with the 2019-nCoV\_N1 (N1) and 2019-nCoV\_N2 (N2) primer-probe sets to investigate whether differences in sensitivity could lead to inconclusive results. **(A)** We determined the difference in Ct values between N1 and N2 primer probe sets for all tested clinical samples. **(B)** We compared Ct values obtained with the two primer-probe sets for clinical samples with Ct values higher than 35. **(C)** We evaluated outcomes of the US CDC assay based on N1 and N2 at two different cut-off levels (Ct = 40 or 38). We found that N2 has a broader range of Ct values between 40-45, whereas N1 only detected Ct values just above 40. We conclude that these differences do not affect the overall performance of the US CDC assay as the percentage of inconclusive samples is below 3% for cut-off values of 40 or more strictly 38 Ct. N1 = 2019-nCoV\_N1, N2 = 2019-nCoV\_N2, ND = not detected.

#### Lower sensitivity of RdRp-SARSr (Charité) primer-probe set

To further investigate the relatively low performance of the RdRp-SARSr (Charité) primer-probe set, we compared our standardized primer-probe concentrations with the recommended concentrations in the confirmatory (Probe 1 and Probe 2) and discriminatory (Probe 2 only) RdRp-SARSr (Charité) assays. We deviated from the recommended concentrations in the original assays to make a fair comparison across primer-probe sets, using 500 nM of each primer and 250 nM of probe 2. To investigate the effect of primer-probe concentration on the ability to detect SARS-CoV-2, we made a direct comparison between **(1)** our standardized primer (500 nM) and probe (250 nM) concentrations, **(2)** the recommended concentrations of 600 nM of forward primer, 800 nM of reverse primer, and 100 nM of probe 1 and 2 (confirmatory assay), and **(3)** the recommended concentrations of 600 nM of forward primer, 800 nM of reverse primer, and 200 nM of probe 2 (discriminatory assay) per reaction<sup>5</sup>. We found that adjusting the primer-probe concentrations or using the combination of probes 1 and 2 did not increase SARS-CoV-2 RNA detection when using 10-fold serial dilutions of our RdRp RNA transcripts, or full-length SARS-CoV-2 RNA from cell culture (**Fig. 5**). The Charité Institute of Virology Universitätsmedizin Berlin assay is designed to use the E-Sarbeco primer-probes as an initial screening assay, and the RdRp-SARSr primer-probes as a confirmatory test<sup>5</sup>.

Our data suggest that the RdRp-SARSr assay is not a reliable confirmatory assay at low SARS-CoV-2 amounts.

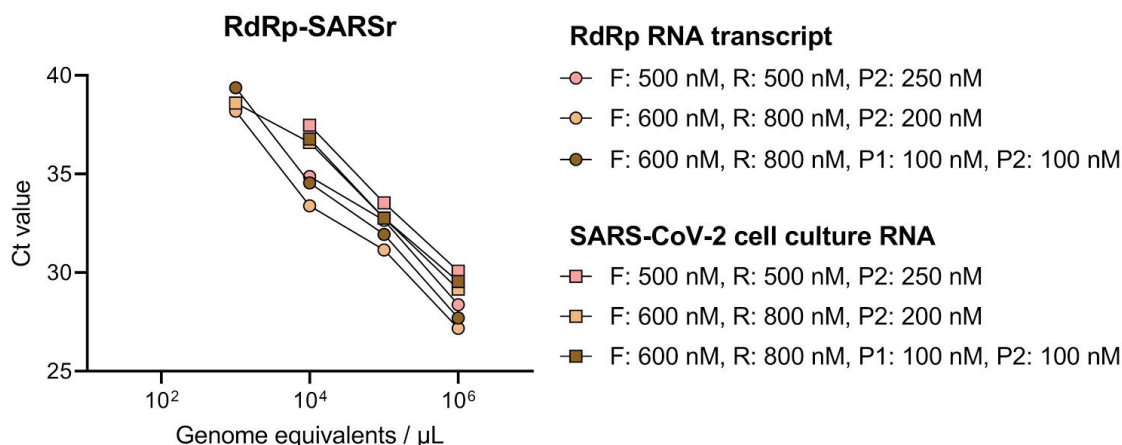


**Fig 5: No effect of different concentrations of RdRp-SARSr primers and probes on analytical sensitivity.** Low performance of the standardized RdRp-SARSr primer-probe set triggered us to further investigate the effect of primer concentrations. We compared our standardized primer-probe concentrations (500 nM of forward and reverse primers, and 250 nM of probe) with the recommended concentrations in the confirmatory assay (600 nM of forward primer, 800 nM of reverse primer, 100 nM of probe 1, and 100 nM of probe 2), and the discriminatory assay (600 nM of forward primer, 800 nM of reverse primer, and 200 nM of probe 2) as developed by the Charité Institute of Virology Universitätsmedizin Berlin. Standard curves for both RdRp-transcript standard and full-length SARS-CoV-2 RNA are similar, which indicates that higher primer concentrations did not improve the performance of the RdRp-SARSr set. Symbol indicates tested sample type (circles = RdRp transcript standard, and squares = full-length SARS-CoV-2 RNA from cell culture) and colors indicate the different primer and probe concentrations.

### Mismatches in primer binding regions

As viruses evolve during outbreaks, nucleotide substitutions can emerge in primer or probe binding regions that can alter the sensitivity of PCR assays. To investigate whether this had already occurred during the early COVID-19 pandemic, we calculated the accumulated genetic diversity from 992 available SARS-CoV-2 genomes (**Fig. 6A**) and compared that to the primer and probe binding regions (**Fig. 6B**). Thus far we detected 12 primer-probe nucleotide mismatches that have occurred in at least two of the 992 SARS-CoV-2 genomes.

The most potentially problematic mismatch is in the RdRp-SARSr reverse primer (**Fig. 6B**), which likely explains our sensitivity issues with this set (**Figs. 2, 3, 6**). Oddly, the mismatch is not derived from a new variant that has arisen, but rather that the primer contains a degenerate nucleotide (S, binds with G or C) at position 12, and 990 of the 992 SARS-CoV-2 genomes encode for a T at this genome position (**Fig. 6B**). This degenerate nucleotide appears to have been added to help the primer anneal to SARS-CoV and bat-SARS-related CoV genomes<sup>5</sup>, seemingly to the detriment of consistent SARS-CoV-2 detection. Earlier in the outbreak, before hundreds of SARS-CoV-2 genomes became available, non-SARS-CoV-2 data were used to infer genetic diversity that could be anticipated during the outbreak. As a result, several of the primers contain degenerate nucleotides

**(Supplemental Table 3).** For RdRp-SARSR, adjusting the primer (S→A) may resolve its low sensitivity.

Of the variants that we detected in the primer-probe regions, we only found four in more than 30 of the 992 SARS-CoV-2 genomes (>3%, **Fig. 6B**). Most notable was a stretch of three nucleotide substitutions (GGG→AAC) at genome positions 28,881-28,883, which occur in the three first positions of the CCDC-N forward primer binding site. While these substitutions define a large clade that includes ~13% of the available SARS-CoV-2 genomes and has been detected in numerous countries<sup>14</sup>, their position on the 5' location of the primer may not be detrimental to sequence annealing and amplification. The other high frequency variant that we detected was T→C substitution at the 8<sup>th</sup> position of the binding region of the 2019-nCoV\_N3 forward primer, a substitution found in 39 genomes (position 28,688). While this primer could be problematic for detecting viruses with this variant, the 2019-nCoV\_N3 set has already been removed from the US CDC assay. We found another seven variants in only five or fewer genomes (<0.5%, **Fig. 6B**), and their minor frequency at present does not pose a major concern for viral detection. This scenario may change if those variants increase in frequency: most of them lie in the second half of the primer binding region, and may decrease primer sensitivity<sup>15</sup>. The WA1\_USA strain (GenBank: MN985325) that we used for our comparisons did not contain any of these variants.

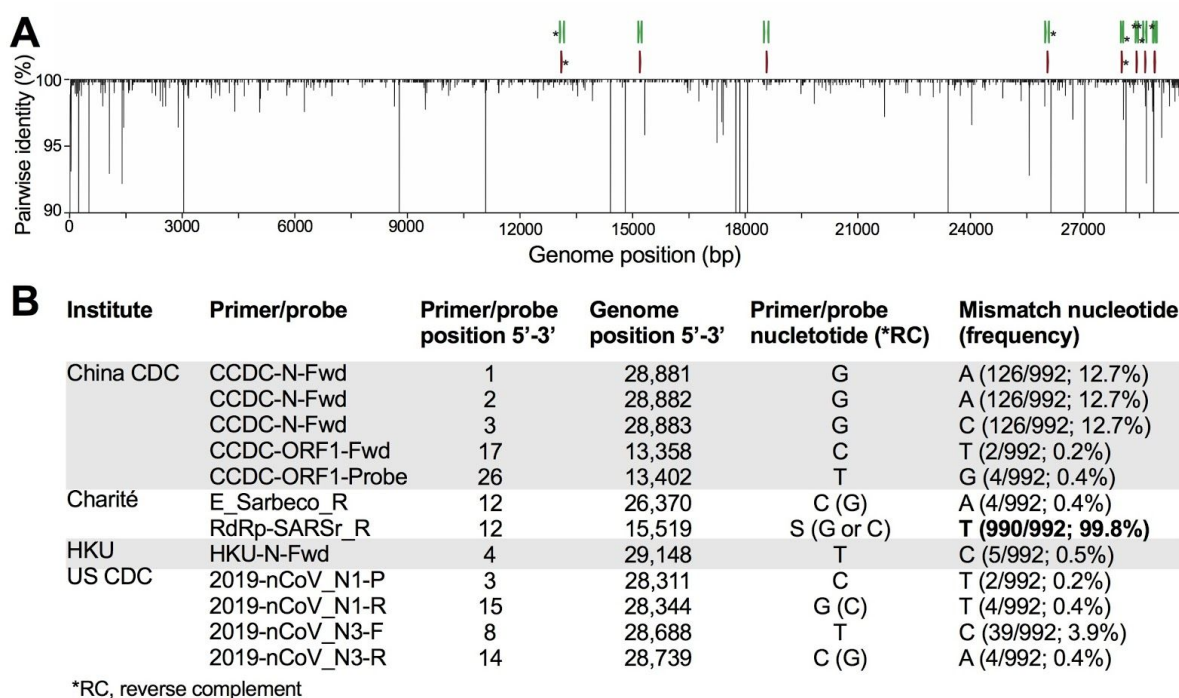


**Fig. 6: High frequency primer and probe mismatches may result in decreased sensitivity for SARS-CoV-2 detection.** (A) We aligned nucleotide diversity across 992 SARS-CoV-2 genomes sequenced up to 22 March 2020 and determined mismatches with the nine primer-probe sets. We measured diversity using pairwise identity (%) at each position, disregarding gaps and ambiguous nucleotides. Asterisks (\*) at the top indicate primers and probes targeting regions with one or more mismatches. Genomic plots were designed using DNA Features Viewer in Python<sup>16</sup>. (B) We only listed mismatch nucleotides with frequencies above 0.1%. These mismatches may result in decreased sensitivity of primer-probe sets.

## Discussion

Our comparative results of primer-probe sets used in qRT-PCR assays indicate some variation in the analytical sensitivities for SARS-CoV-2 detection and ability to differentiate between true negatives and positives at low RNA concentrations. We found that the most sensitive primer-probe sets are E-Sarbeco (Charité), HKU-ORF1 (HKU), HKU-N (HKU), and 2019-nCoV\_N1 (US CDC), which could partially (63-75%) detect SARS-CoV-2 at 10 virus copies per  $\mu\text{L}$  of RNA. In contrast, the RdRp-SARSr (Charité) primer-probe set had the lowest sensitivity, as also shown by an independent study<sup>13</sup>, likely stemming from a mismatch in the reverse primer. Furthermore, we found background cross-reactivity when testing nasopharyngeal swabs prior to the COVID-19 pandemic using the China CDC and US CDC assays. While the China CDC “N” and “ORF1” primer-probe sets require further investigation, we found that the background cross-reactivity did not affect the outcomes of the US CDC assay when testing clinical samples from the COVID-19 pandemic. Overall, our findings indicate that the qRT-PCR assay from HKU, the screening assay (E-Sarbeco) from Charité, and the updated assay from the US CDC are most reliable for accurate detection of SARS-CoV-2.

The exact cause of the background cross-reactivity when testing clinical samples from pre-COVID-19 respiratory disease patients using the China CDC and US CDC primer-probe sets is unknown. One possibility is that these primers and probes can slightly amplify other seasonal coronaviruses. We did not detect cross-reactivity when using the Charité and HKU sets, and indeed, the assay developers reported that the primers and probes did not detect other circulating coronaviruses and respiratory viruses<sup>4,5</sup>. Cross-reactivity with other viruses would severely limit the utility of any assay and requires further investigation.

Our study does have several limitations to consider. First, we standardized PCR conditions to make a fair comparison between primer-probes sets used in four common qRT-PCR assays for detection of SARS-CoV-2. By standardizing the concentration of primers and probes, PCR kits, and thermocycler conditions, we deviated from the conditions as recommended by each assay which may have influenced our findings. For instance, we selected an annealing temperature of  $55^{\circ}\text{C}$  which was lower than recommended for the assays developed by Charité ( $58^{\circ}\text{C}$ )<sup>5</sup> and HKU ( $60^{\circ}\text{C}$ )<sup>4</sup>, but similar to the assay developed by US CDC ( $55^{\circ}\text{C}$ )<sup>6</sup>. No specific PCR conditions were reported for the assay developed by the China CDC<sup>7</sup>. The two assays (Charité and HKU) with higher annealing temperatures did not yield background amplification, which suggests that our standardized annealing temperature likely did not have a large effect on our findings. Second, when determining the sensitivity of primer-probe sets, we performed eight replicates at low concentrations of SARS-CoV-2 RNA spiked into (pre-COVID-19) clinical samples. While we evaluated the US CDC using 172 clinical samples collected during the COVID-19 pandemic, more replicates for the other assays are required to accurately determine the lower detection limit. Importantly, sensitivity as reported in our study may not be applicable to other PCR kits or thermocyclers; analytical sensitivities and positive-negative cut-off values should be locally validated when establishing these assays.

## Methods

## Ethics

Residual de-identified nasopharyngeal samples collected during 2017 (pre-COVID-19) were obtained from the Yale-New Haven Hospital Clinical Virology Laboratory. In accordance with the guidelines of the Yale Human Investigations Committee (HIC), this work with de-identified samples is considered non-human subjects research. These samples were used to create the mock substrate for the SARS-CoV-2 spike-in experiments (**Fig. 3**). Clinical samples from COVID-19 patients during March 2020 at the Yale-New Haven Hospital were collected in accordance to the HIC-approved protocol #2000027690. These samples were used to test the US CDC 2019-nCoV\_N1 and 2019-nCoV\_N2 primer-probe sets (**Fig. 4**).

## Generation of RNA transcript standards

We generated RNA transcript standards for each of the five genes targeted by the diagnostic qRT-PCR assays using T7 transcription. A detailed protocol can be found here<sup>10</sup>. Briefly, cDNA was synthesized from full-length SARS-CoV-2 RNA (WA1\_USA strain from UTMB; GenBank: MN985325). Using PCR, we amplified the nsp10, RdRp, nsp14, E, and N genes with specifically designed primers (**Supplemental Table 1**). We purified PCR products using the Mag-Bind TotalPure NGS kit (Omega Bio-tek, Norcross, GA, USA) and quantified products using the Qubit High Sensitivity DNA kit (ThermoFisher Scientific, Waltham, MA, USA). We determined fragment sizes using the DNA 1000 kit on the Agilent 2100 Bioanalyzer (Agilent, Santa Clara, CA, USA). After quantification, we transcribed 100-200 ng of each purified PCR product into RNA using the Megascript T7 kit (ThermoFisher Scientific). We quantified RNA transcripts using the Qubit High sensitivity RNA kit (ThermoFisher Scientific) and checked quality using the Bioanalyzer RNA pico 6000 kit. For each of the RNA transcript standards (**Supplemental Table 2**), we calculated the number of genome copies per  $\mu\text{L}$  using Avogadro's number. We generated a genomic annotation plot with all newly generated RNA transcript standards and the nine tested primer-probe sets based on the NC\_045512 reference genome using the DNA Features Viewer Python package (**Fig. 1A**)<sup>16</sup>. We generated standard curves for each combination of primer-probe set with its corresponding RNA transcript standard (**Fig. 1B**), using standardized qRT-PCR conditions as described below.

## qRT-PCR conditions

To make a fair comparison between nine primer-probe sets (**Table 1**), we used the same qRT-PCR reagents and conditions for all comparisons. We used the Luna Universal One-step RT-qPCR kit (New England Biolabs, Ipswich, MA, USA) with standardized primer and probe concentrations of 500 nM of forward and reverse primer, and 250 nM of probe for all comparisons. PCR cycler conditions were reverse transcription for 10 minutes at 55°C, initial denaturation for 1 min at 95°C, followed by 40 cycles of 10 seconds at 95°C and 20 seconds at 55°C on the Biorad CFX96 qPCR machine (Biorad, Hercules, CA, USA). We calculated analytical efficiency of qRT-PCR assays tested with corresponding RNA transcript standards using the following formula<sup>17,18</sup>:

$$E = 100 \times (10^{-1/\text{slope}} - 1)$$

## Validation with SARS-CoV-2 RNA and mock samples

We prepared mock samples by extracting RNA from 12 de-identified nasopharyngeal swabs collected in 2017 (pre-COVID-19) from hospital patients with respiratory disease using the MagMAX Viral/Pathogen Nucleic Acid Isolation kit (ThermoFisher Scientific) following manufacturer's protocol. We used 300  $\mu$ L of sample and eluted in 75  $\mu$ L. After nucleic acid extraction, we pooled eluates from 12 patients and spiked these mock samples with 10-fold dilutions of SARS-CoV-2 RNA. We compared analytical efficiency and sensitivity of qRT-PCR assays by testing 10-fold dilutions ( $10^6$ - $10^0$  genome equivalents/ $\mu$ L) of SARS-CoV-2 RNA as well as the SARS-CoV-2 RNA-spiked mock samples, in duplicate. In addition, we determined analytical sensitivity of the nine primer-probe sets by testing 6-8 replicates of high dilutions of SARS-CoV-2 RNA-spiked mock samples ( $10^2$ - $10^0$  genome equivalents/ $\mu$ L) and mock samples without addition of RNA.

### **Clinical samples**

Clinical samples from COVID-19 diagnosed patients were obtained from the Yale-New Haven Hospital. We extracted nucleic acid from nasopharyngeal swabs, saliva, urine, and rectal swabs using the MagMax Viral/Pathogen Nucleic Acid Isolation kit following manufacturer's protocol. We used 300  $\mu$ L of each sample and eluted in 75  $\mu$ L. We used the Luna Universal One-step RT-qPCR kit with standardized primer and probe concentrations of 500 nM of forward and reverse primer, and 250 nM of probe for the 2019-nCoV\_N1, 2019-nCoV\_N2, and RP (human control) primer-probe sets to detect SARS-CoV-2 in each sample. PCR cycler conditions were reverse transcription for 10 minutes at 55°C, initial denaturation for 1 min at 95°C, followed by 45 cycles of 10 seconds at 95°C and 20 seconds at 55°C on the Biorad CFX96 qPCR machine (Biorad, Hercules, CA, USA).

### **Mismatches in primer binding regions**

We investigated mismatches in primer binding regions by calculating pairwise identities (%) for each nucleotide position in binding sites of assay primers and probes. Ignoring gaps and ambiguous bases, we compared all possible pairs of nucleotides in all columns of a multiple sequence alignment including all available SARS-CoV-2 genomes (as of 22 March 2020). We assigned a score of 1 for each identical pair of bases, and divided the final score by the total number of valid nucleotide pairs, to finally express pairwise identities as percentages. Pairwise identity of less than 100% indicates mismatches between primers or probes and some SARS-CoV-2 genomes. We calculated mismatch frequencies and reported absolute and relative frequencies for mismatches with frequency higher than 0.1%. The DNA Features Viewer package in Python was used to generate the diversity plot (**Fig. 5**)<sup>16</sup>.

### **Acknowledgements**

We thank K. Plante and the University of Texas Medical Branch World Reference Center for Emerging Viruses for providing SARS-CoV-2 RNA, the Yale COVID-19 Laboratory Working Group for technical support, P. Jack and S. Taylor for discussions, and A. Greninger for feedback on a previous version of this manuscript. This research was funded by the generous support from the Yale Institute for Global Health and the Yale School of Public Health start-up package provided to NDG. CBFV is supported by NWO Rubicon 019.181EN.004.

## References

1. Gorbalenya, A. E. *et al.* Severe acute respiratory syndrome-related coronavirus: The species and its viruses – a statement of the Coronavirus Study Group. *bioRxiv* 2020.02.07.937862 (2020) doi:10.1101/2020.02.07.937862.
2. Wu, F. *et al.* A new coronavirus associated with human respiratory disease in China. *Nature* **579**, 265–269 (2020).
3. Zhou, P. *et al.* A pneumonia outbreak associated with a new coronavirus of probable bat origin. *Nature* **579**, 270–273 (2020).
4. Chu, D. K. W. *et al.* Molecular Diagnosis of a Novel Coronavirus (2019-nCoV) Causing an Outbreak of Pneumonia. *Clin. Chem.* (2020) doi:10.1093/clinchem/hvaa029.
5. Corman, V. M. *et al.* Detection of 2019 novel coronavirus (2019-nCoV) by real-time RT-PCR. *Euro Surveill.* **25**, (2020).
6. CDC. Coronavirus Disease 2019 (COVID-19). *Centers for Disease Control and Prevention* <https://www.cdc.gov/coronavirus/2019-ncov/lab/rt-pcr-panel-primer-probes.html> (2020).
7. Institute of Viral Diseases. China CDC. *National Institute for Viral Disease Control and Prevention* [http://ivdc.chinacdc.cn/kyjz/202001/t20200121\\_211337.html](http://ivdc.chinacdc.cn/kyjz/202001/t20200121_211337.html) (2020).
8. WHO - Coronavirus disease (COVID-19) technical guidance: Laboratory testing for 2019-nCoV in humans. <https://www.who.int/emergencies/diseases/novel-coronavirus-2019/technical-guidance/laboratory-guidance>.
9. Harcourt, J. *et al.* Severe Acute Respiratory Syndrome Coronavirus 2 from Patient with 2019 Novel Coronavirus Disease, United States. *Emerg. Infect. Dis.* **26**, (2020).
10. Vogels, C. B. F., Fauver, J. R., Ott, I. & Grubaugh, N. D. Generation of SARS-CoV-2 RNA transcript standards for qRT-PCR detection assays v1 (protocols.io.bdv6i69e). (2020) doi:10.17504/protocols.io.bdv6i69e.
11. Svec, D., Tichopad, A., Novosadova, V., Pfaffl, M. W. & Kubista, M. How good is a PCR efficiency estimate: Recommendations for precise and robust qPCR efficiency assessments. *Biomol Detect Quantif* **3**, 9–16 (2015).
12. CDC Revises SARS-CoV-2 Assay Protocol; Surveillance Testing on Track to Start Next Week. *360Dx* <https://www.360dx.com/pcr/cdc-revises-sars-cov-2-assay-protocol-surveillance-testing-track-start-next-week>.
13. Casto, A. M. *et al.* Comparative Performance of SARS-CoV-2 Detection Assays using Seven Different Primer/Probe Sets and One Assay Kit. *medRxiv* (2020) doi:10.1101/2020.03.13.20035618.
14. Genomic epidemiology of novel coronavirus. *Nextstrain* [https://nextstrain.org/ncov?c=gt-ORF14\\_50](https://nextstrain.org/ncov?c=gt-ORF14_50).
15. Bru, D., Martin-Laurent, F. & Philippot, L. Quantification of the detrimental effect of a single primer-template mismatch by real-time PCR using the 16S rRNA gene as an example. *Appl. Environ. Microbiol.* **74**, 1660–1663 (2008).
16. Zulkower, V. & Rosser, S. DNA Features Viewer, a sequence annotations formatting and plotting library for Python. *bioRxiv* 2020.01.09.900589 (2020) doi:10.1101/2020.01.09.900589.
17. Broeders, S. *et al.* Guidelines for validation of qualitative real-time PCR methods.

*Trends Food Sci. Technol.* **37**, 115–126 (2014).

18. Ginzinger, D. G. Gene quantification using real-time quantitative PCR: an emerging technology hits the mainstream. *Exp. Hematol.* **30**, 503–512 (2002).



## Supplement

**Supplemental Table 1:** Primers for generation of T7 RNA transcript standards for SARS-CoV-2.

Target	Primer	Sequence
nsp10	nsp10-Std-T7-Fwd	TAATACGACTCACTATAGGGGTGGGGGACAACCAATCACT
	nsp10-Std-Rev	AGACGAGGTCTGCCATTGTG
RdRp	RdRp-Std-T7-Fwd	TAATACGACTCACTATAGGGAATAGAGCTCGCACCGTAGC
	RdRp-Std-Rev	CATCTACAAAACAGCCGGCC
nsp14	nsp14-Std-T7-Fwd	TAATACGACTCACTATAGGGTAGTGCTAAACCACCGCCTG
	nsp14-Std-Rev	AACTGCCACCATCACAACCA
E	E-Std-T7-Fwd	TAATACGACTCACTATAGGGGCGTGCCTTTGTAAGCACAA
	E-Std-Rev	GGCAGGTCCTTGATGTCACA
N	N-Std-T7-Fwd	TAATACGACTCACTATAGGGGAATTGTGCGTGGATGAGGC
	N-Std-Rev	TGTCTCTGCGGTAAGGCTTG

**Supplemental Table 2: RNA transcript standards for common SARS-CoV-2 diagnostic assays (see genomic context on Figure 1A).**

Gene	Length	Sequence
nsp10	704nt (13,122 - 13,825)	GUGGGGGACAACCAAUCACUAAUUGUGUUAGAUGUUGUGUACA CACACUGGUACUGGUCAGGCAAUAACAGUUACACCGGAAGCCAAU AUGGAUCAAGAAUCCUUUGGUGGUGCAUCGUGUUGUCUGUACUG CCGUUGCCACAUGAUAUCCAAAUCCUAAAAGGAUUUUUGACUU AAAAGGUAAGUAUGUACAAAUACCUACAACUUGUGCUAAUGACCC UGUGGGUUUUACACUUAAAAACACAGUCUGUACCGUCUGCGGUA UGUGGAAAGGUUAUGGUCUGUAGUUGUGAUAACUCCGCGAACCC AUGCUUCAGUCAGCUGAUGCACAAUCGUUUUUAAACGGGUUUGC GGUGUAAGUGCAGCCCGUCUUACACCGUGCGGCACAGGCACUAG UACUGAUGUCGUUAACAGGGCUUUUGACAUCUACAAUGAUAAGU AGCUGGUUUUGCUAAAUUCCUAAAAACUAAUUGUUGUCGUUCCA AGAAAAGGACGAUGAUGACAUUUAAUUGAUUCUUAUUUGAGU UAAGAGACACACUUUCUCUAAUACCUACCAACUAUGAAGAAUUAU AAUUUACUUAAGGAUUGUCCAGCUGUUGCUAAACAUGACUUCUUU AAGUUUAGAAUAGACGGUGACAUGGUACCACAUUAUACACGUCAA CGUCUUACUAAAUACACAAUGGCAGACCUCGUCU
RdRp	883nt (15,094 - 15,976)	AAUAGAGCUCGCACCGUAGCUGGUGUCUCUAUCUGUAGUACUUAU GACCAAUAGACAGUUUCAUAAAAUUAAUUGAAAUCAAUAGCCGC CACUAGAGGAGCUACUGUAGUAAUUGGAACAAGCAAUUUCUUAUGG UGGUUGGCACAACAUGUUAAAAACUGUUUAUJAGUGAUGUAGAAAA CCCUCACCUUAUGGGUUGGGAUUAUCCUAAAUGUGAUAGAGCCA UGCCUAAACAUGCUUAGAAUUUAGGCCUCACUUGUUCUUGCUCGC AAACAUAACAACGUGUUGUAGCUUGUCACACCGUUUCUUAUAGAUUA GCUAAUGAGUGUGUCUCAAGUAUUGAGUGAAAUGGUC AUGUGUGG CGGUUCACUUAUGUUAACCAGGUGGAACCUCUACAGGAGAUGC CACAACUGCUUAUGCUAAUJAGUGUUUUUAAACAUUUGUCAAGCUGU CACGGCCAAUGUUAAUGCACUUUUUAUCUACUGAUGGUAACAAAAU UGCCGAUAAGUAUGUCCGCAUUUUAACAACACAGACUUUAUGAGUG UCUCUAUAGAAAUAGAGAUGUUGACACAGACUUUGUGAAUGAGUU UUACGCAUAAUUUGCGUAAACAUUUCUCAAUGAUGAUACUCUCUGA CGAUGCUGUUGUGUGUUCAAUAGCACUUUAUGCAUCUCAAGGUC UAGUGGCUAGCAUAAAGAACUUUAAGUCAGUUCUUUAUUUAUCAA ACAAUGUUUUUUAUGUCUGAAGCAAUUGUUGGACUGAGACUGACC UUACUAAAGGACCUC AUGAAUUUUGCUCUCAACAUAACA AUGCUAG UUAAACAGGGUGAUGAUUAUGUGUACCUUCCUUAACCCAGAUCUAA CAAGAAUCCUAGGGGCCGGCUGUUUUGUAGAUG
nsp14	848nt (18,447- 19,294)	UAGUGCUAAACCACCGCCUGGAGAUCAAUUUAACACCUCUACUACC ACUUAUGUACAAAGGACUUCUUUGGAAUGUAGUGCGUAUAAAGAU UGUACAAUUGUUAAGUGACACACUUAAAAUCUCUCUGACAGAGU CGUAUUUGUCUUUAGGGCACAUGGCUUUGAGUUGACAUCUAUGA AGUAUUUUGUGAAAAUAGGACCUGAGCGCACCUGUUGUCUUAUGU GAUAGACGUGCCACAUGCUUUUCCACUGCUUCAGACACUUUAUGCC UGUUGGCAUCAUUCUUAUUGGAUUUGAUUACGUCUUAUAAUCCGUU UAUGAUUGAUGUUAACAAGGGGUUUUACAGGUAACCUACAAG CAACCAUGAUCUGUAUUGUCAAGUCCAUGGUAUUGCACAUGUAGC UAGUUGUGAUGCAAUCAUGACUAGGUGUCUAGCUGUCCACGAGU GCUUUGUUAAGCGUGUUGACUGGACUAUUGAAUAUCCUUAUAAU GGUGAUGAACUGAAGAUUAUUGCGGCUUUGUAGAAAGGUUCAACAC AUGGUUGUUAAGCUGCAUUUAUAGCAGACAAAUCCAGUUCUU CACGACAUUGGUAACCCUAAAGCUAUUAAGUGUACCUACAAGCU GAUGUAGAAUGGAAGUUCUAUGAUGCACAGCCUUGUAGUGACAAA GCUUAUAAAAUAGAAGAAUUAUUCUUAUUCUUAUGCCACACAUUCU GACAAAUUCACAGAUGGUGUAUGCCUAAUUUUGAAUUGCAAUGUC GAUAGAUUACCUUGCUAAUUCUUAUUGUUUGUAGAUUUUGACACUAGA GUGCUAUCUAAACCUAACUUGCCUGGUUGUGAUGGUGGCAGUU
Envelope (E)	808nt (26,207 -	GCGUGCCUUUGUAAGCACAAGCUGAUGAGUACGAACUUAUGUAC UCAUUCGUUUCGGAAGAGACAGGUACGUUAUAGUUAUAGCGUA

27,116) CUUCUUUUUCUUGCUUUCGUGGUAUUCUUGCUAGUUACACUAGC  
CAUCCUUACUGCGCUUCGAUUGUGUGCGUACUGCUGCAAUUAUUG  
UUAACGUGAGUCUUGUAAAACCUUCUUUUUACGUUUACUCUCGUG  
UUAAAAUCUGAAUUCUUCUAGAGUUCUGAUUCUUCUGGUCUAAA  
CGAACUAAAUAUUUAUUAGUUUUUCUGUUUGGAACUUUAAUUUU  
AGCCAUGGCAGAUUCCAACGGUACUAAUACCGUUGAAGAGCUUAA  
AAAGCUCUUUGAACAAUGGAACCUAGUAAUAGGUUUCCUUAUCCU  
UACAUGGAUUUGUCUUCUACA AUUUUGCCU AUGCCAACAGGAAUAG  
GUUUUUUGUAUAUAUUUAAGUUAAUUUUUCCUCUGGCUGUUAUGGC  
CAGUACUUUAGCUUGUUUUGUGCUUGCUGCUGUUUACAGAAUA  
AAUUGGAUCACCGGUGGAAUUGCUAUCGCAUUGGCUUGUCUUGU  
AGGCUUGAUGUGGCUCAGCUACUUAUUGCUUCUUCAGACUGU  
UUGCGCGUACGCGUUCUUGUGGUCUUAUCCAGAAACUAACA  
UUCUUCUCAACGUGCCACUCCAUGGCACUUAUCUGACCAGACCGC  
UUCUAGAAAGUGAACUCGUAUUCGGAGCUGUGAUCCUUCGUGGA  
CAUCUUCGUUUUGCUGGACACCAUCUAGGACGCUGUGACAUCAA  
GGACCUGCC

Nucleocapsid (N) 1363nt  
(28,068 -  
29,430)

GAAUUGUGCGUGGAUGAGGCUGGUUCUAAAUCACCCAUUCAGUA  
CAUCGAUAUCGGUAAUUAACAGUUUCCUGUUUACCUUUUACAAU  
UAAUUGCCAGGAACCUAAAUUGGGUAGUCUUGUAGUGCGUUGUU  
CGUUCUAUGAAGACUUUUUAGAGUAUCAUGACGUUCGUGUUGUU  
UUAGAUUUCAUCUAAACGAACAACUAAAUGUCUGAUAAUGGAC  
CCAAAAUCAGCGAAAUGCACCCCGCAUUACGUUUGUGGACCCU  
CAGAUUCAACUGGCAGUAACCAGAAUGGAGAACGCAGUGGGCG  
CGAUCAAAACAACGUCGGCCCCAAGGUUUACCCAUAUACUGCG  
UCUUGGUUCACCGCUCUCACUCAACAUGGCAAGGAAGACCUUAAA  
UCCUCGAGGACAAGGCGUUCCAAUUAACACCAAUAGCAGUCCA  
GAUGACCAAUUGGCUACUACCGAAGAGCUACAGACGAAUUCGU  
GGUGGUGACGGUAAAUGAAAGAUCUCAGUCCAAGAUGGUUUU  
CUACUACCUAGGAACUGGGCCAGAAGCUGGACUUCUUAUGGUG  
CUAACAAAGACGGCAUCAUAUGGUUGCAACUGAGGGAGCCUUG  
AAUACACCAAAAAGAUACAUAUUGGCACCCGCAAUCCUGCUAACA  
GCUGCAAUCGUGCUACAACUUCUCAAGGAACAACAUUGCCAAAA  
GGCUUCUACGCAGAAGGGAGCAGAGGCGGCAGUCAAGCCUCUUC  
UCGUUCCUCAUCACGUAGUCGCAACAGUUAAGAAAUUCAACUCC  
AGGCAGCAGUAGGGGAACUUCUCCUGCUAGAAUGGCUGGCAAUG  
GCGGUGAUGCUGCUCUUGCUUUGCUGCUGCUUGACAGAUUGAAC  
CAGCUUGAGAGCAAAAUGUCUGGUAAAAGGCCAACAAACAAGGC  
CAAACUGUCACUAAGAAAUCUGCUGCUGAGGCUUCUAAGAAGCCU  
CGGCAAAAACGUACUGCCACUAAAGCAUACAUAUGUAACACAAGCU  
UUCGGCAGACGUGGUCCAGAACAACCCAAAGGAAUUUUUGGGGA  
CCAGGAACUAUUCAGACAAGGAACUGAUUACAACAUAUGGCCGCA  
AAUUGCACAUAUUGCCCCAGCGCUUCAGCGUUCUUCGGAUUGU  
CGCGCAUUGGCAUGGAAGUCACACCUUCGGGAACGUGGUUGACC  
UACACAGGUGCAUCAAAUUGGAUGACAAAGAUCCAAUUUCAA  
GAUCAAGUCAUUUUGCUGAAUAAGCAUAUUGACGCAUACAACA  
UCCCACCAACAGAGCCUAAAAGGACAAAAAGAAGGCGUGAU  
GAAACUCAAGCCUUAACCGCAGAGACA

**Supplemental Table 3:** Degenerate bases in common SARS-CoV-2 qRT-PCR assay primers and probes.

Primer	Degenerate base, and its purpose	Position in primer (5'-3')	Genomic position (5'-3')	Pairing base in genomes (frequency)
RdRp-SARSr-F	R, to pair with T or C	5	15,435	T (992/992; 100.0%)
RdRp-SARSr-R	<b>S, to pair with C or G</b>	12	15,519	T (990/992; 99.8%)
RdRp-SARSr-R	R, to pair with T or C	3	15,528	T (992/992; 100.0%)
HKU-ORF1-F	Y, to pair with A or G	6	18,783	A (992/992; 100.0%)
HKU-ORF1-F	R, to pair with T or C	12	18,789	T (989/992; 99.7%)
HKU-ORF1-P	W, to pair with T or A	13	18,861	T (992/992; 100.0%)
HKU-ORF1-R	R, to pair with T or C	4	18,906	T (992/992; 100.0%)
2019-nCoV_N3-P	Y, to pair with A or G	2	28,705	A (992/992; 100.0%)